



Physical modeling of the dynamics of a revetment breakwater built on reclaimed coral calcareous sand foundation in the South China Sea—tsunami wave

Kunpeng He^{1,2} · Jianhong Ye¹

Received: 30 July 2020 / Accepted: 2 February 2021 / Published online: 22 February 2021
© Springer-Verlag GmbH Germany, part of Springer Nature 2021

Abstract

In this study, taking the reclamation engineering in the South China Sea as the background, several wave flume experiments (geometrical similarity scale is set as 1:10) are performed to study the dynamics and the stability of a reclaimed calcareous sand foundation and the breakwater built on it, under the impacting of tsunami wave. Tsunami wave is similarly simulated by N wave in the wave flume. It is shown by the experimental results that the revetment breakwater has no visible displacement, and there is no significant deformation in the reclaimed coral sand foundation, regardless the foundation is in dense or loose state under tsunami wave attacking. Furthermore, there is indeed excess pore pressure generated in the reclaimed coral foundation with a maximum magnitude of 1.5 kPa, caused by the water overtopping or the seepage. It is found that the excess pore pressure has not caused liquefaction in the reclaimed calcareous sand foundation due to the fact that there is only one peak impacting for the tsunami wave-induced load, rather than a cyclic one. Finally, it is concluded that the reclaimed calcareous sand foundation and the breakwater built on it are basically stable under tsunami wave impacting. However, the excessive water overtopping would be a potential threat for the vegetation behind the breakwater, as well as for the underground desalinated water in the reclaimed lands.

Keywords Stability of breakwater · Reclaimed calcareous sand foundation · Revetment breakwater · South China Sea · Tsunami wave · Wave flume test

Introduction

Tsunami is a type of ocean wave propagating in ocean with a long wavelength. After a tsunami wave is triggered, it can travel several thousands of kilometers accompanied with little energy attenuation in deep sea if there is no blocking effect of island groups or large shoals. When a tsunami wave arrives at a shallow water area on continental shelf, its energy will gradually concentrate. Its wave height becomes higher and higher as the seawater gets shallower. This kind of great wave will bring great threat to the lives and property safety in coastal areas; e.g., more than 280,000 people died in the countries

around the Indian Ocean because a great tsunami was triggered by a very strong earthquake ($M_w = 9.1$) that occurred off the coast of Sumatra on December 26, 2004 (Satake et al. 2005). Another $M_w = 9.0$ strong earthquake has occurred off the east coast of Japan on March 11, 2011. The great tsunami caused by this earthquake also had a devastating impact on the countries around the Pacific Ocean, especially Japan. As a result, more than 18,000 people died or missed (Ranghieri and Ishiwatari 2008; Gu 2011).

The South China Sea (SCS) is an important transportation channel for the world trade and energy transportation. In order to conduct scientific research, ocean observation, marine rescue, and to guarantee the aviation safety, a series of artificial lands have been successfully built with coral calcareous sand. In order to avoid the direct scouring to the reclaimed artificial lands by ocean waves, and enhance the stability of these artificial lands, a large number of revetment breakwaters were built on the outer margins of the artificial lands. Research work conducted by Takagi and Bricker (2014) had shown that breakwaters could play an important

✉ Jianhong Ye
Yejianhongcas@gmail.com; Jhye@whrsm.ac.cn

¹ State Key Laboratory of Geomechanics and Geotechnical Engineering, Institute of Rock and Soil Mechanics, Chinese Academy of Sciences, Wuhan 430071, China

² University of Chinese Academy of Sciences, Beijing 100049, China

role in reducing the impact of tsunami wave on coastal structures. In the ocean environment, whether a tsunami would occur or not in the South China Sea is an important issue worthy of our attention. In 2006, USGS conducted a hazard assessment of potential earthquake sources in the Pacific region. USGS inferred that the zone along the north-south Manila trench which is at the eastern side of the South China Sea would be a high-risk area (Kirby et al. 2006). Zhou and Adams (1986) pointed out that it is highly possible for a tsunami to occur in the SCS. Sun et al. (2013) found that there was a strong tsunami event that had significantly affected the Xisha Islands in the SCS around 1024 AD. It is indicated that these reclaimed artificial islands in the South China Sea are at great risk of being attacked by tsunami wave during their service periods. The revetment breakwaters built on the reclaimed coral sand foundation are the only engineering structures to ensure the stability of these reclaimed artificial islands. Therefore, it is of great significance to study the stability and dynamics of the revetment breakwater in the SCS under tsunami attract.

Many scholars have carried out a series of works on the stability of breakwater under the impact of tsunami. These works mainly include physical model tests and numerical analysis. On the aspect of physical model tests, Rossetto et al. (2011) proposed a new concept of tsunami wave generation in wave flume to reproduce the great Indian Ocean tsunami that occurred in 2004. Tanimoto et al. (1984) carried out some large-scale wave flume tests to generate solitary waves to impact a vertical breakwater. Based on the experimental results, they proposed a formulation to estimate the magnitude of impact pressure on breakwater applied by tsunami wave. Ikeno et al. (2001); Ikeno and Tanaka (2003) further improved the Tanimoto's formulation by introducing some parameters considering the wave breaking. Esteban et al. (2008, 2009, 2012) proposed a design formulation for caisson breakwaters under the action of tsunami based on laboratory tests. Mikami et al. (2015) conducted some wave flume tests to study the effect of a detached breakwater on tsunami along a coastal line. Hanzawa et al. (2012a) proposed a method to analyze the interaction between tsunami waves and rubble mound breakwaters adopting wave flume tests. Guler et al. (2015) analyzed the interaction between tsunami waves and a rubble mound breakwater by establishing a scaled physical model for the Haydarpasa port in Istanbul, Turkey. However, the seepage, overflow, and other important factors affecting the stability of breakwaters have not been considered in these studies. Sassa et al. (2016) developed a new centrifuge experimental system in which the tsunami-induced overflow seepage could be coupled. They found that the coupled overflow-seepage behavior of tsunami could significantly promote the development of scouring for the gravels mound behind a breakwater. The wave flume tests conducted by Takahashi et al. (2014) indicated that the tsunami-induced seepage would

reduce the bearing capacity of foundation. Mizutani and Imamura (2000) conducted several physical model tests to investigate the tsunami-induced overflow over a quay wall. They also proposed a set of formulations to estimate the maximum wave impact on the surface behind levees. However, there is a common shortcoming in these flume experiments mentioned above. The deformable seabed foundation of breakwaters was not considered when evaluating the stability of breakwaters under the action of tsunami.

There were also a number of important works that have been conducted on the aspect of numerical modeling. Hanzawa et al. (2012b) analyzed the wave pressure on a detached breakwater under the action of solitary waves by adopting the numerical model CADMAS-SURF. Guler et al. (2018) adopted the IHFOAM solver to analyze the pressure distribution on the surface of a gravel breakwater under the impact of tsunami. However, only the interaction between tsunami wave and breakwaters was analyzed in most previous works, and the role of seabed foundation was not considered. Miyake et al. (2009) performed some centrifugal model tests for a caisson breakwater impacted by a great tsunami; then, Imase et al. (2012) further performed a numerical simulation for these model tests adopting the smoothed particle hydrodynamic (SPH) method. Based on their works, it was found that the seepage force in the rubble mound is considerable during the tsunami impacting. Sawada and Miyake (2015) evaluated the stability of a breakwater impacted by a tsunami especially considering the seepage force by the discrete element method. It was shown by their work that the tsunami-induced seepage force would reduce the safety of breakwaters. The works on numerical modeling mentioned above have successfully revealed the interaction between tsunami waves and structures such as breakwaters from the perspective of CFD. However, the deformable seabed foundation is also not taken into consideration in computation as well.

Currently, it has been widely recognized that there are three types of failure mode for the wave-induced failure of offshore breakwaters. They are (1) excessive residual horizontal displacement of breakwaters due to slipping, referred as mode I; (2) overturning of breakwaters due to the huge wave impact, referred as mode II; (3) partial or complete loss of the bearing capacity of seabed foundation due to the softening or liquefaction, referred as model III (Sumer 2009; Teh et al. 2003; Chavez et al. 2017). Due to the fact that the seabed foundation of a breakwater is not or cannot be taken into consideration in some numerical modelings or physical model tests, the safety of breakwaters can be only checked adopting the failure mode I and failure mode II in most previous works and in some currently implemented national design codes, e.g., the Chinese code of design and construction of breakwater (JTS154-1-2011 2011). Actually, the wave, breakwaters, and their foundation are coupled system in ocean environment. The foundation of a breakwater plays an important role

in guaranteeing the stability of the breakwater. Engineering survey for breakwater failure shows that about 60–70% of failure cases have close relationship with the softening and liquefaction of foundation due to the pore pressure accumulation under cyclic wave loading. Therefore, the evaluation of the safety of a breakwater is not reliable if the foundation of the breakwater is not taken into consideration, whether the adopted method is numerical modeling or physical model test.

In order to overcome the shortcomings that the seabed foundation cannot be considered in previous numerical models, Ye et al. (2013a, b) successfully developed an integrated numerical model FSSI-CAS 2D/3D, in which the fluid-structure-seabed interaction can be taken into consideration. This numerical model is able to evaluate the stability of offshore structures under the impact of various ocean waves. Additionally, this model has been successfully applied to study the dynamic response of seabed foundation, and the stability of breakwaters under the impact of solitary wave (Ye et al. 2013c). Previous studies have shown that N waves are more similar to real tsunami waves than the solitary waves (Tadepalli and Synolakis 1994). Unfortunately, the wave maker in FSSI-CAS 2D/3D cannot generate an N wave at present.

In this study, taking the reclamation engineering in the South China Sea as the engineering background, the dynamic response and the stability of the reclaimed calcareous sand foundation and the revetment breakwater built on it under tsunami wave, rather than random wave (Zhang and Ye 2021), are studied by conducting several groups of large-scale model tests. The physical model is established in a wave flume adopting a geometrical scale of 1:10. N wave is generated in the wave flume to simulate tsunami wave during the tests. The wave pressure on the revetment breakwater, the displacement of breakwater, and the pore pressure in the reclaimed coral sand foundation are recorded. Different tidal levels and dry densities of the coral sand foundation are considered in tests. The test results could be a solid basis for further works and provide some valuable references for the design as well as the past-construction maintenance of the revetment breakwaters built on the reclaimed coral reef islands in the South China Sea.

Experimental setups

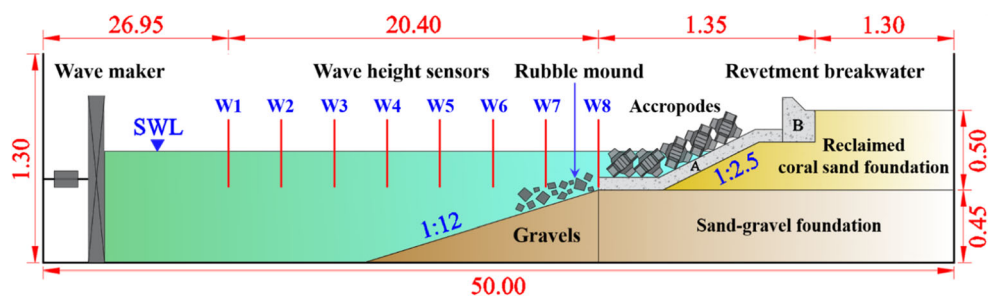
The length of the wave flume is 47 m, the height is 1.3 m, and the width is 1.0 m. Due to the limited height of the wave flume, it is impossible to physically simulate the overall slope of the natural coral reefs which generally are up to several thousand meters high in the ocean. A possible approach is to only focus on the interaction between tsunami wave, the revetment breakwater, and its reclaimed coral sand foundation; and we only pay attention on the displacement of the breakwater, the settlement, and the deformation of the reclaimed

coral sand foundation under tsunami wave load. Therefore, the physical model in the wave flume only includes the revetment breakwater, the coral calcareous sand foundation, and the reef flat in this study.

The physical model is constructed according to a geometric similarity scale of 1:10. The schematic map of the test model constructed in the wave flume is illustrated as Fig. 1. In this model, the revetment breakwater consists of two parts, a revetment and a vertical caisson. Both parts of the revetment breakwater are made of concrete. For the simplicity, the revetment is referred to as structure A, and the vertical caisson is referred to as structure B in the following analysis. The foundation behind and below the breakwater is built with coral calcareous sand over the original calcareous deposits, which is modeled with the sand-gravel mixture in the physical model. In engineering practice, the revetment breakwater is usually covered by a great number of accropodes to dissipate the wave energy. Correspondingly, some small accropodes also have been made according to the geometric similarity scale and they are laid on the revetment breakwater in the physical model, as shown in Fig. 1. Hydrological parameters are determined based on the long-term observation in the South China Sea in the past 20 years. The elevation of extreme high water level is set as +2.3 m above the average sea level ± 0 m in the practical engineering design. According to the distance from the water level to the top of the vertical caisson, the water depth in the wave flume for the extreme high and average water level is determined as 0.71 m and 0.48 m in tests by applying this geometrical similarity scale 1:10.

The distance from the left side of the revetment breakwater to the wave maker is about 47.25 m. Eight wave profile sensors labeled as W1 to W8 are installed at typical positions in the wave flume. Location of these water profile sensors are shown as Table 1. The revetment breakwater and accropodes model are made of C50 concrete, which are the same as that used at in-site. The reclaimed foundation is made using coral calcareous sand sampled from a reclaimed coral reef island in the South China Sea. The original soil layer beneath the reclaimed coral sand foundation is modeled with the mixture of quartz sand and gravels. The mass ratio of quartz sand to gravel is set as 1.6:1 to ensure that the permeability coefficient of the mixture is close to that of the original soil layer. Gravels with a particle size range of 1–2 cm are used to model the reef flat. It is worth noting that the real micro-topography of reef flat is complicated (uneven and rough). It has significant effect on the wave propagation and the wave energy dissipation. However, the complicated micro-topography of reef flat is impossible to be reproduced accurately in the physical mode. The upper surface of the gravels in the physical model is also rough and uneven, which could simulate the reef flat in the aspect of absorbing wave energy to some extent. The mechanical parameters of the materials used in the physical model are listed in Table 2.

Fig. 1 Schematic map of the test model constructed in the wave flume (unit: m) (note: the revetment is labeled as A, and the vertical caisson is labeled as B)



Totally 14 pore pressure sensors are buried in the reclaimed coral sand foundation and sand-gravel mixture layer. Twenty-three wave impact sensors are uniformly fixed on the upper surface of structures A and B, and two resistance-type displacement transducers are fixed horizontally and vertically on the top of structure B, as shown in Fig. 2. The parameters of these sensors used in test are listed in Table 3. It is noted that all the sensors are installed along the longitudinal central axis of the wave flume, far away from the lateral glass of the wave flume to avoid the adverse effect of lateral boundaries.

In order to precisely control the dry density of the soil foundation under revetment breakwater, this test model is built layer by layer with the help of a plate-type vibrator which could ensure that the dry density of each layer reaches its expected value. In this process, these pore water pressure sensors are buried in their preset positions. The completed physical model with and without accropodes is shown in Fig. 3 and Fig. 4.

Actually, there is no tight and rigid connection between the revetment breakwater model and the lateral glass of the wave flume. As a consequence, the movement of the revetment breakwater model along the wave flume direction is not constraint, while the movement of the revetment breakwater perpendicular to the wave flume is completely constraint by the stiff lateral glass of the wave flume. This type of lateral boundary condition is similar with that under the condition of plane strain. As we know, the revetment breakwater around these reclaimed lands in the South China Sea (SCS) is a type of linear engineering structure. In this study, only a typical section of these revetment breakwaters and their reclaimed coral sand foundation in the South China Sea is taken as the object. This is also the typical condition of plane strain. Therefore, the lateral boundary condition of the physical model is highly similar to that at engineering in-sites in the SCS.

As a type of special material, calcareous coral sands are mainly consist of calcium carbonate and magnesium carbonate.

Table 1 Location of the wave profile sensors (horizontal distance to the wave maker)

Sensor no.	W1	W2	W3	W4	W5	W6	W7	W8
Location (m)	26.95	29.95	32.95	35.95	38.95	41.95	44.67	47.35

It is mainly located in the zone from 30° north latitude to 30° south latitude, widely distributed in the South China Sea (SCS), the Western Continental Shelf of India, the Northeast and Northwest Continental Shelf of Australia, and the Caribbean Sea. The calcareous coral sand particles have the characteristics of significant surface roughness, containing inner porosity, irregular shape, easy breakage, and etc., making its engineering mechanical properties different with that of the conventional terrestrial quartz sand. In recent decade, a number of laboratory works have been performed to study the behavior of calcareous coral sand (He et al. 2020a, b; Gao and Ye 2019; Wang et al. 2019). The basic properties of the coral sand sampled from the SCS used in test are also measured in this study, as listed in Table 4. Its gradation curve is demonstrated in Fig. 5.

The main purpose of this work is to experimentally evaluate the dynamics and stability of the revetment breakwater in the South China Sea under the action of tsunami wave. Besides, this study also would like to explore the effect of some factors, such as the usage of accropodes, tidal level, and the dry density of the reclaimed coral sand foundation on the stability of the revetment breakwater. Therefore, the test conditions of two dry densities of the reclaimed coral sand foundation, two water depths, two wave heights, and the usage of accropodes or not are set in the tests, as illustrated in Table 5.

Laboratory generation of tsunami wave

Solitary wave was widely used to approximately simulate the tsunami wave in most previous literature in the past. However, more and more observations on seismic tsunamis, such as the Nicaragua tsunami that occurred in 1993 and the Jave (Indonesia) tsunami that occurred in 1994, have indicated that tsunami wave is composed of a great crest and a trough, which is similar to the character “N”. Tadepalli and Synolakis (1994) named such a wave as N wave, and proposed a general mathematical expression for N wave for the first time. According to many scientific reports on tsunami, lots of witnesses had seen the seawater receding on beach before a tsunami arriving. The classical theory of solitary wave could not explain this phenomenon. However, it was well explained adopting the N wave theory, as shown in Fig. 6 (a). For the earthquakes that occurred in deep sea, especially the earthquakes due to the

Table 2 Mechanical parameters of the materials used in the physical model

Material	Elasticity modulus (MPa)	Permeability (m/s)	D_{50} (mm)
Concrete	350	0	-
Calcareous sand	20	2.0×10^{-5}	0.54
Mixture of sand-gravel	30	6.8×10^{-4}	2
Gravel	50	1.0×10^{-2}	15

relative dislocation between the upper wall and the foot wall of a giant fault, N wave is generally formed on the surface of sea water (Synolakis 1999). Therefore, N wave can simulate the characteristics of tsunami wave better than solitary wave in most cases. In this study, N wave is generated by the wave maker in the wave flume.

Tadepalli and Synolakis (1996) proposed the general expression of the wave profile for N wave:

$$\eta(x, 0)/d = \varepsilon \frac{H}{d} (x-x_2) \operatorname{sech}^2(k(x-x_1)) \tag{1}$$

$$k = \sqrt{3H/(4d^3)} \tag{2}$$

where d is the water depth; H is the height of tsunami wave; ε is a scale parameter used to ensure the wave height is equal to H . The distance $L = x_2 - x_1$ is used to reflect the horizontal scale of N waves.

The effect of x_1, x_2 on the shape of N waves is demonstrated in Fig. 6 (b). It is observed that the crest and trough of N waves are changed with different $L = x_2 - x_1$; and the amplitude of crest is equal to the amplitude of trough when $L = x_2 - x_1 = 0$. Otherwise, the amplitude of crest is significantly greater than that of trough if $L = x_2 - x_1 > 0$ for N waves.

N wave is selected to simulate the tsunami in this laboratory study. At the beginning of testing, the input parameters for the wave maker are constantly adjusted, ensuring that the generated N waves meet the requirement of wave height and wave shape. As shown in Fig. 7, the profiles of the waves generated

in the flume are compared with the theoretical profiles of N waves. It is observed that the wave generated in the flume is in good agreement with the theoretical wave profile at the crest and trough zone in time domain. An interesting phenomenon which can be observed in Fig. 7 is that there are some continuous oscillations at the trough of the generated wave. The reason is that after the crest and trough of an N wave are generated, the water in front of the wave maker inevitably vibrates freely even though the plate of the wave maker stops moving. This continuous oscillation is impossible to be eliminated in the flume at present. Therefore, it can be accepted that the shape and characteristics of the waves generated in the wave flume are highly similar to N waves. The simulation of tsunami wave in this laboratory study is successful.

Result analysis

Due to the fact that a tsunami wave with a great height would bring great threat to the stability of a breakwater, no accropode is laid in front of the breakwater at the time when astronomical tide is occurring. Based on this recognition, test 5 is taken as the typical test to analyze the dynamics and the stability of the revetment breakwater which is built on the artificial reef island. Other tests will be used to explore the effect of wave height, water depth, dry density, and the usage of accropodes on the dynamics and stability of the revetment breakwater under tsunami wave.

Fig. 2 Schematic of the location of the 11 pore pressure sensors, 23 pressure sensors, and 2 displacement sensors (LVDT) in the physical model (unit: m)

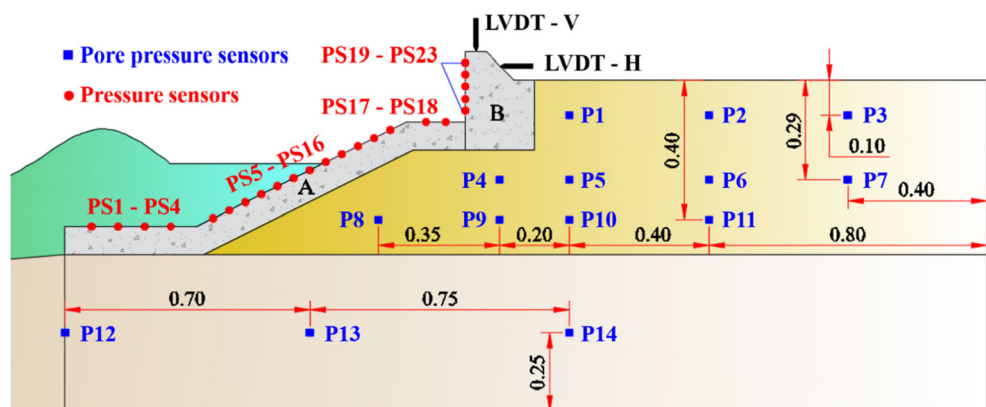


Table 3 Parameters of the sensors used in the tests

Sensor type	Measurement range	Resolution	Accuracy (FS*)
Wave profile sensors	±500 mm	1 mm	0.1%
Displacement sensors	±25 mm	0.01 mm	0.1%
Pore pressure sensors	10-100 kPa	0.1 Pa	0.3%
Pressure sensors	10 kPa	0.1 Pa	0.5%

*FS full scale

Wave profiles

The wave profiles recorded at W1 to W8 in test 5 are shown in Fig. 8. As can be seen in Fig. 8, partial reflection occurs and the reflected wave propagates in the opposite direction in the wave flume. Intensive collision and partial superposition occur between the incident waves and reflected waves at position W8. Another phenomenon can be seen in Fig. 8 that the wave height of incident waves is gradually increasing on the gravel slope due to the gradual reducing of water depth. It can be easily recognized that the wave energy will be dissipated when the tsunami wave is propagating on the rough surface of the gravel slope. Besides, seepage also inevitably occurs in the porous gravel slope during the propagation of tsunami wave, which will consume the wave energy as well. However, the wave height of incident wave indeed is increasing on the gravel slope under the combined effect of these factors in this test. Thus, a recognition that can be obtained is that the effect of topography of the gravel slope is more important than the other factors on the profile of tsunami wave.

Displacement of breakwater and overtopping

Displacement is a direct indicator to assess the stability of the revetment breakwater. The horizontal motion and vertical settlement of structure B are shown in Fig. 9. As illustrated in Fig. 9, the displacement of breakwater is very small and could be ignored. During the impact by the tsunami wave, the breakwater is pushed to the right side by a certain magnitude of horizontal force. At this moment, passive soil pressure is generated in the reclaimed coral sand foundation to resist the rightward movement of the breakwater. It can be known from the perspective of the final displacement of the breakwater that there is no passive shear failure that occurred in the coral sand foundation. Therefore, it could be concluded that this breakwater can basically keep stable with the strong support supplied by the calcareous sand behind it.

When the tsunami wave impacts structure B, the incident waves are partially reflected. At the meantime, overtopping occurs over structure B, as shown in Fig. 10. Some water pass over the top of structure B, and fall directly on the surface of the reclaimed coral sand foundation behind the breakwater;

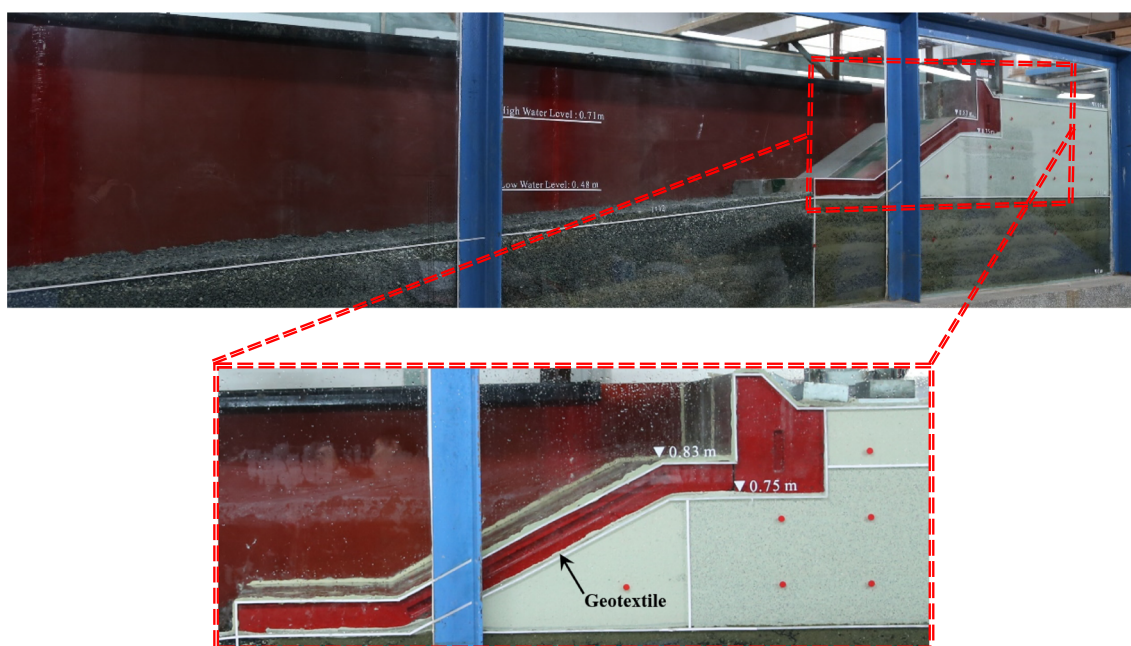


Fig. 3 A real view of the physical model for the revetment breakwater and its coral sand foundation (note: geotextile is laid between the breakwater and the coral sand foundation to avoid the loss of sand particles caused by wave scouring)

Fig. 4 A real view of the accropodes installed on the revetment in the completed physical model



then, the overtopped water permeates downward slowly in the coral sand foundation. The total mass of the overtopped water recorded in test 5 is 1.45kg per sectional meter.

Based on the observation in this test, it is found that the revetment breakwater does not slip, and the foundation behind the breakwater is not damaged under the action of the tsunami wave. The reclaimed coral sand foundation and the revetment breakwater built on it are both stable. It is worth noting that the sea water passing over the breakwater cannot be discharged back to the sea due to the blocking of structure B. The overtopped sea water will lead to fatal ecological disasters, such as the death of vegetation behind the revetment breakwater and pollution of the desalinated underground water in these reclaimed artificial lands.

Pore pressure in coral sand foundation

The dynamic response of pore pressure directly affects the strength of the reclaimed coral sand foundation below and behind the revetment breakwater. The residual pore pressure would lead to the reduction of effective stress, resulting in the softening or liquefaction of sand foundation. In this section, the physical mechanism of the behavior of the reclaimed coral calcareous sand foundation will be further revealed by analyzing the dynamic response of pore pressure. The dynamic response of pore pressure measured by the 13 pore pressure sensors is shown in Fig. 11.

As shown in Fig. 11, the pore pressure in the reclaimed coral sand foundation, as well as beneath the original coral reef soil layer, increases rapidly at the beginning stage under the tsunami wave impacting. Then, the pore pressure dissipates gradually during the process of the water surface calming down. The increasing and dissipation rates of pore pressure are both increasing with the buried depth in the reclaimed coral sand foundation. Pore pressures recorded at P1, P4, P8, and P12 are higher than that recorded at the other positions with the same elevation, due to the fact that these sensors are buried near to the revetment breakwater. P12 is buried in the original deposited soil layer, where the permeability coefficient is high. This is the reason why the pore pressure recorded at P12 oscillates greatly and dissipates rapidly. The maximum residual pore pressure recorded at P12 is about 1.5kPa.

There is an important phenomenon that needs to be noted that P1 is buried 0.2 m above P5, and 0.14 m above the static water level (SWL); however, the maximal dynamic pore pressure recorded at P1 is about 0.25kPa which is greater than the peak pore pressure recorded at P5. There are totally three types of mechanism that could make the pore pressure in the coral sand foundation change significantly, as illustrated in Fig. 12: (1) The overtopped water flowing over structure B permeates downward after falling on the surface of the coral sand foundation behind structure B; (2) plastic deformation has occurred in the coral sand foundation. (3) The static water levels in the coral sand foundation slightly rise due to the water

Table 4 Basic physical properties of the coral sand used in this study

Specific gravity (G_s)	Maximum dry density (ρ_{max})	Minimum dry density (ρ_{min})
2.83	1540 kg/m ³	1250 kg/m ³

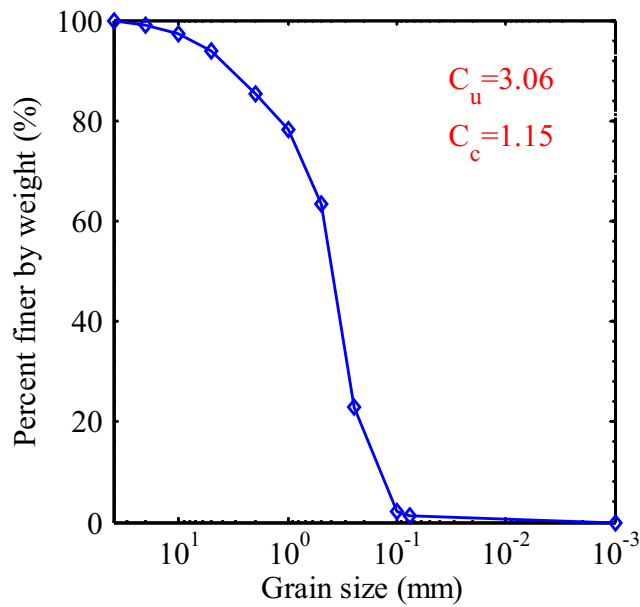


Fig. 5 Gradation curve of the coral sand sampled from the SCS used in this study

seepage from the water domain to the coral sand foundation through the sand-gravel mixture below.

As illustrated in Fig. 2, the pore pressure sensors P1, P2, and P3 are over the static water level by 14cm. The initial pore pressure should be zero. Even though the static wave level has

raised due to the third mechanism stated above, it is impossible to rise by 14cm (note: the pore pressure at P4 only rises maximally by about 0.2kPa, and it is indicated that the static water level only rises by about 2cm). Therefore, the pore pressure sensors P1, P2, and P3 are still not merged by the pore water in the coral sand foundation. Even though plastic deformation has occurred, the pore pressure at P1, P2, and P3 should be zero if there is no wave overtopping occurring in the test. On the contrary, it is observed that there is dynamic pore pressure at P1, P2, and P3 in the test, as clearly shown in Fig. 11. Finally, it is known that the dynamic pore pressure at P1, P2, and P3 is mainly caused by the water overtopping.

Another interesting phenomenon that could be observed in Fig. 11 is that the time period for the pore pressure reaching its peak value at P4, P8, and P12 is much shorter than that at P1 where the dynamic pore pressure is mainly caused by the water overtopping. Therefore, the dynamic pore pressure at P8 and P12 is mainly caused by the above-stated third mechanism related to the water seepage through the sand-gravel mixture. The dynamic pore pressure at P4 is firstly caused by the water seepage, latterly significantly affected by the permeating overtopped water. In Fig. 11, it seems that the dynamic pore pressures at P5, P6, P7, P9, P10, and P11 in the coral sand foundation are also mainly affected by the permeating overtopped water.

Table 5 Test conditions considering the dry density, tsunami wave parameters, and the wave energy dissipation measurement

Test no.	Dry density* (kg/m ³)	Water level (m)	Wave height (m)	Accropodes
1	1320	0.48	0.15	No
2	1500	0.48	0.15	No
3	1320	0.71	0.19	No
4	1320	0.71	0.19	Yes
5	1500	0.71	0.19	No
6	1500	0.71	0.19	Yes

* It is the dry density of the coral sand foundation of the revetment breakwater

Fig. 6 Comparison of the theoretical wave profile between a third-order solitary wave and an *N* wave (Grimshaw 1971), and the effect of x_1, x_2 on the shape of *N* wave

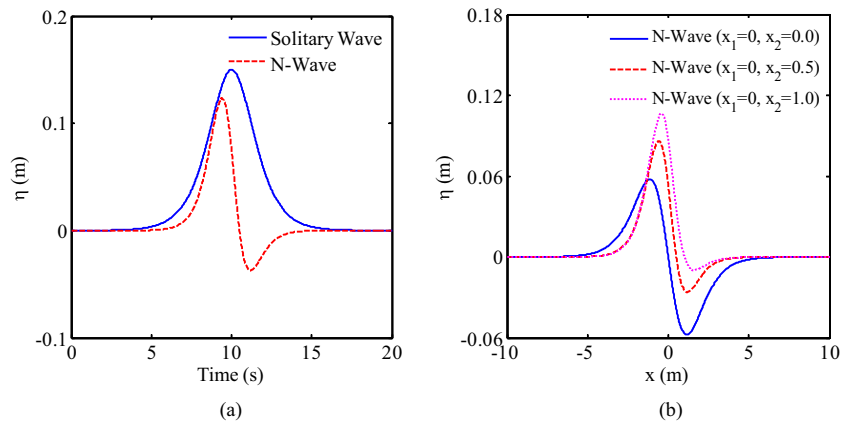
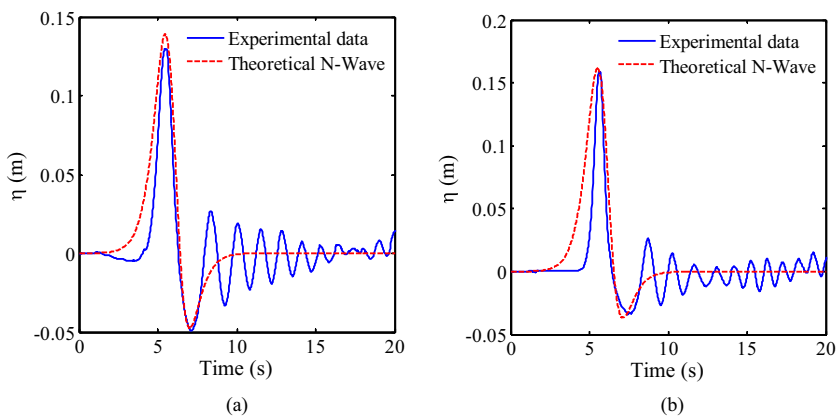


Fig. 7 Comparison of the wave profiles between the waves generated in the flume and the theoretical *N* waves. (a) Test 1 ($H=0.15$ m, $D=0.48$ m) (b) Test 3 ($H=0.19$ m, $D=0.71$ m)



Impact pressure on the revetment breakwater

Stability of the revetment breakwater will be directly affected by the impact pressure of tsunami wave. In this section, four typical locations are selected as the representatives to analyze the impact pressure induced by the tsunami wave on the revetment breakwater. The time history of the tsunami wave-induced impact pressure measured in test 5 is shown in Fig. 13.

It can be seen in Fig. 13 that the time history of the tsunami wave-induced impact pressure has only one impacting peak, and this impacting peak is followed by some oscillations. The shape of the impacting peak combining the first followed trough is similar with the *N* wave generated in the wave flume in this test. The time duration of the impacting peak zone is decreasing gradually from PS3 to PS20, which indicates that the action time of the tsunami wave on the breakwater is decreased along the surface of structures A and B. This phenomenon has the typical characteristics of impact pressure.

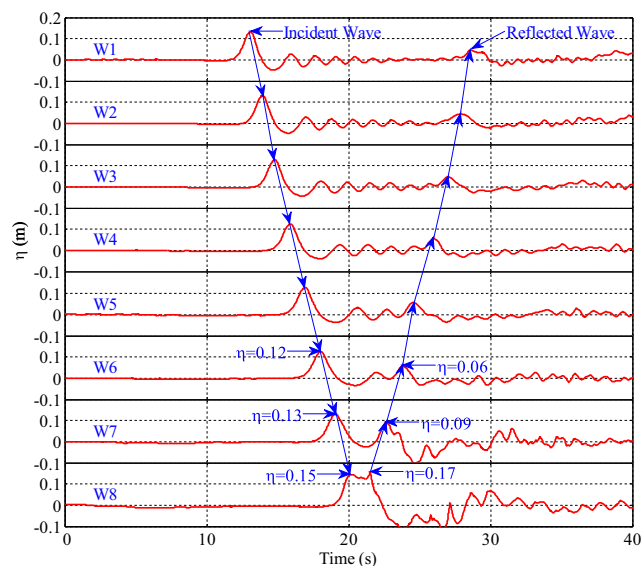


Fig. 8 Wave profiles recorded at W1 to W8 in test 5

Distribution of the maximum wave impact on the surface of the revetment breakwater is shown in Fig. 14. The maximum wave impact is 2.59 kPa on the slope of structure A. On the surface of structure B, the maximum wave impact is only 1.52 kPa, which is significantly less than that on structure A. It is indicated that there is wave energy dissipation during the tsunami wave climbing on structure A. These characteristics are beneficial to the stability of structure B.

The tsunami wave impact force acted on structures A and B is shown in Fig. 15. The maximum impact force on structure A is about 0.6kN/m in horizontal and 0.35kN/m in vertical. The maximum impact force on structure B is about 0.45kN/m in horizontal. Based on the observation in this test, no failure has been observed. Horizontal and vertical displacement of the revetment breakwater are both less than 0.1 mm, as shown in Fig. 9. It can be concluded that the revetment breakwater is basically stable under this tsunami wave impacting due to the strong support supplied by the passive soil pressure of calcareous sand behind the revetment breakwater.

Analysis of affecting factors

Previous studies have shown that the tidal level, the density of foundation, and the usage of accropodes would have some effects on the stability of a breakwater. This section is aimed

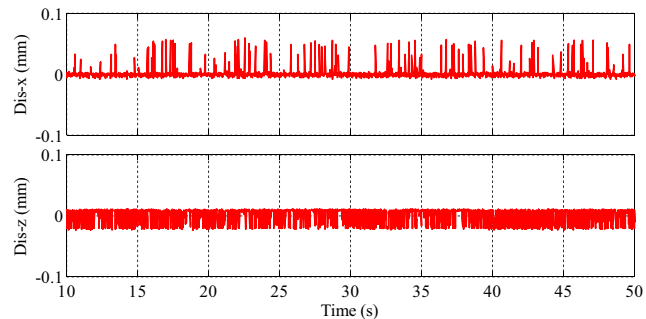


Fig. 9 Time history of the horizontal and vertical displacement of structure B in test 5

Fig. 10 Revetment breakwater is impacted by a tsunami wave and the overtopping occurred in test 5. (a) Lateral view (b) Longitudinal view



at exploring the effects of these factors, respectively on the stability of the revetment breakwater through comparative study.

Effect of accropodes

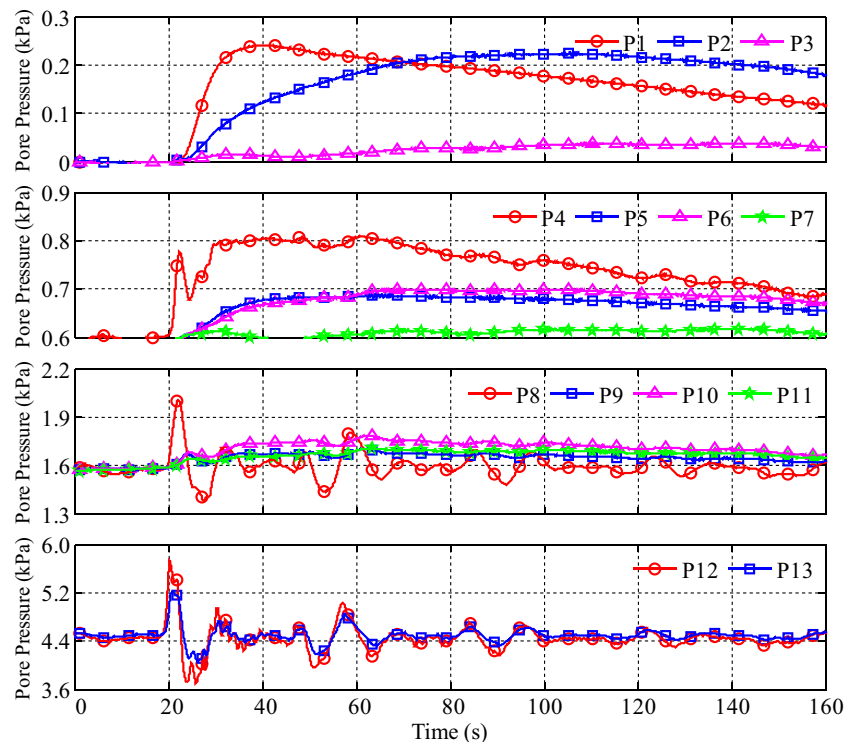
Previous researches have shown that accropodes could contribute much to reducing the impact of waves on breakwater (Ikeno 2001). This section is to explore the effect of the accropodes on enhancing the stability of the revetment breakwater. The water depth and dry density of reclaimed coral sand foundation set in test 6 and test 5 are the same. The difference is that a number of accropodes are used to dissipate the energy of tsunami wave in test 6.

In test 6, the displacement of structure B is also very small, as illustrated in Table 6. More importantly, no overtopping occurred. The distribution of the maximum wave impact on

the surface of structures A and B is shown in Fig. 16. The comparison of the wave force on structures A and B measured in test 5 and test 6 is shown in Fig. 17. As shown in Fig. 16, the maximum wave impact induced by the tsunami wave on structures A and B are 2.32 kPa and 1.07 kPa, respectively in test 5. They are both significantly less than that measured in test 5. It is demonstrated in Fig. 17 that the impact forces on structure A in test 5 and test 6 are basically the same. However, the horizontal impact force on structure B is only 0.15 kN/m in test 6, which is only 1/3 of that measured in test 5. It is indicated that the accropodes can significantly protect structure B under tsunami wave impact, while its protective effects on structure A are general.

The time history of the pore pressures recorded at P1, P4, P8, and P12 in test 5 and test 6 is shown in Fig. 18. The pore pressure recorded at P1 in test 6 is much less than that recorded in test 5. Due to the blocking effect of these accropodes,

Fig. 11 Tsunami-induced pore pressure in the reclaimed coral sand foundation (test 5)



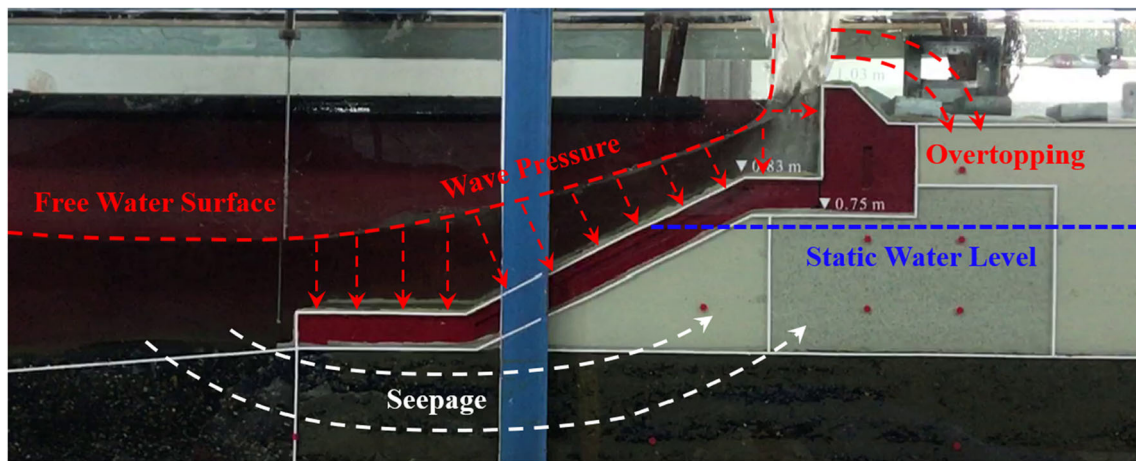


Fig. 12 Mechanism illustration for the change of pore water pressure in the coral sand foundation when the tsunami wave is impacting

wave overtopping is not observed in test 6, while it is observed in test 5, as shown in Fig. 10. It is indicated that the significant pore pressure recorded at P1 in test 5 is mainly caused by the overtopping water. It is found that dynamic response of pore pressure recorded at P8 and P12 is basically the same in test 5 and test 6. Conclusion is drawn that accropodes could contribute much to reduce the pore pressure in the reclaimed coral sand foundation behind structure B. Meanwhile, the excellent consistency of the pore pressure recorded at P8 and P12 in test 5 and test 6 indicates that the wave flume tests performed in this study have a very good repeatability.

Effect of tidal level

Tidal level will be always changed periodically due to the astronomic condition during the service period of the

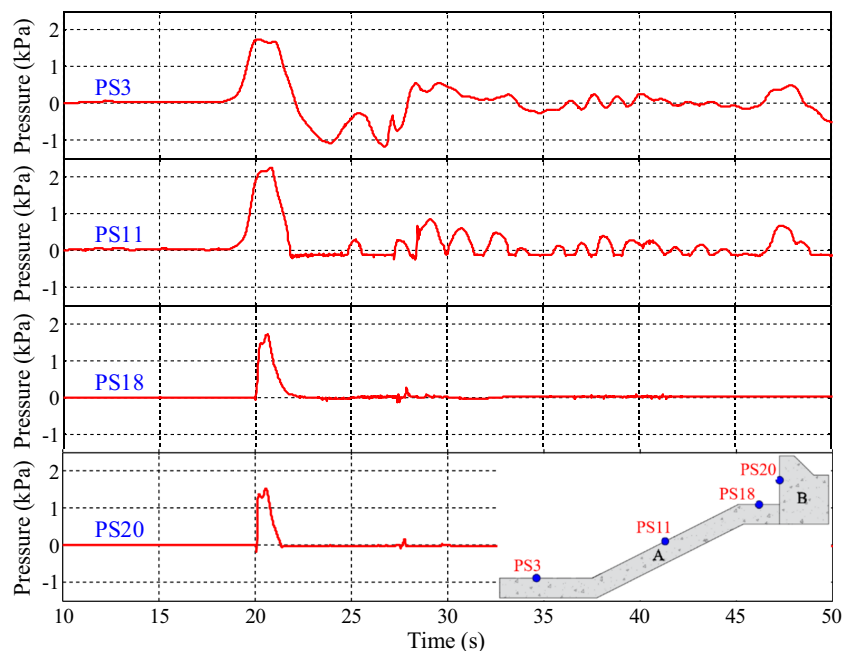
revetment breakwater. There is a direct relationship between the impact of tsunami wave on the revetment breakwater and the tidal level. In this section, the effect of tidal level will be explored by comparing the test results recorded in test 2 ($d = 0.48$ m) and in test 5 ($d = 0.71$ m). In test 2, the distribution of the maximum wave impact on structures A and B is shown in Fig. 19.

It can be seen in Fig. 19 that the wave impact on the surface of structures A and B in test 2 is much less than that recorded in test 5. It is indicated that tsunami wave will bring less threat to the stability of the revetment breakwater at low tide level.

Effect of foundation density

In the practical reclamation engineering in the South China Sea, the compaction degree of the reclaimed coral sand

Fig. 13 Time history of the tsunami wave-induced impact measured in test 5 at four typical positions (hydrostatic pressure is excluded)



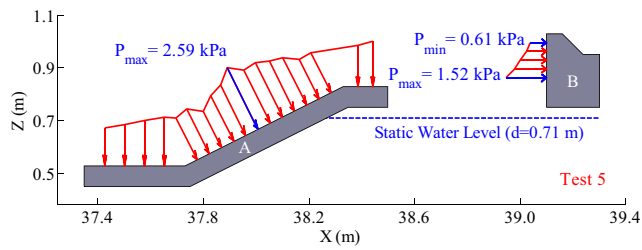


Fig. 14 Distribution of the maximum wave impact on the surface of the revetment breakwater during the tsunami impacting in test 5

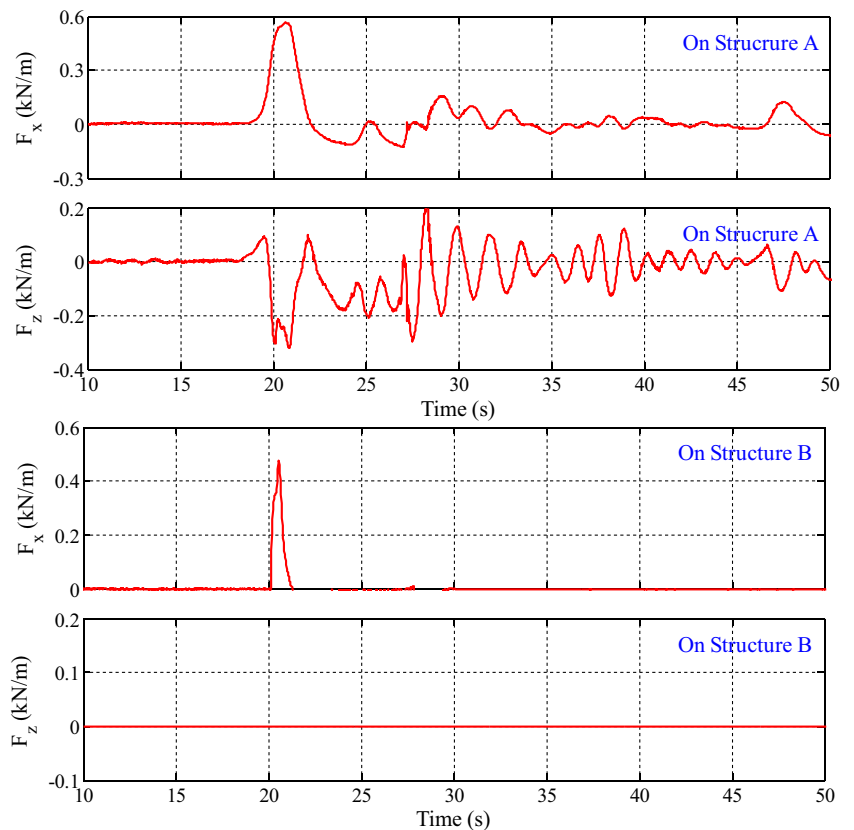
Table 6 Displacement of structure B and the overtopping recorded in test 1 to test 6

Test no.	Test 1	Test 2	Test 3	Test 4	Test 5	Test 6
Displacement x (mm)	0.01	0.01	0.05	0.01	0.05	0.01
Displacement z (mm)	0.01	0.01	0.02	0.01	0.01	0.01
Overtopping (kg/m)	0	0	0	0	1.45	0

foundation may be heterogeneous due to the influence of the construction technology or the limited time for the construction. On the one hand, if the coral sand foundation is loose, the shear strength of the foundation itself is relatively weak. As a result, plastic deformation is easy to occur in the foundation. On the other hand, excess pore pressure is more likely to be accumulated in loose foundation, resulting in the occurrence of softening and liquefaction in the coral sand foundation. It would further lead to failure of the revetment breakwater. In this section, the effect of the dry density of the reclaimed coral sand on the response of pore pressure is studied by comparing the test results recorded in test 3 and test 5. Dry density of the reclaimed coral sand foundation is 1500kg/m^3 in test 5, and 1320kg/m^3 in test 3.

Wave overtopping has not been observed in test 3, and the pore pressures recorded at P1 and P2 are significantly affected by the overtopping in test 5. The pore pressures recorded at P4, P8, P9, and P12 which are under the static water level in the coral sand foundation are selected as the representatives for the comparative analysis. The dynamic response of the pore pressure measured in test 3 and test 5 is shown in Fig. 20. The pore pressure recorded at P4 and P9 shows that the pore pressure in the loose sand foundation increases more rapidly to a much greater magnitude, while the pore pressure dissipates more slowly if the coral sand foundation is dense, due to the fact that the permeability coefficient of dense foundation is less than that of the loose sand foundation. The drainage condition of the coral sand at P8 is limited by structure A, so the dynamic response of the pore pressure recorded

Fig. 15 Time history of the impact force on the breakwater applied by the tsunami wave in test 5 (note: integration of the wave pressure along the surface where wave pressure is applied)



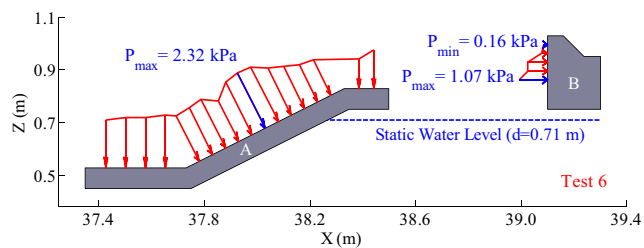


Fig. 16 Distribution of the maximum wave pressure on the surface of the revetment breakwater during the tsunami impacting in test 6 (with accropodes)

at P8 is highly similar in test 5 and test 3. The pore pressure recorded at P12 is basically the same in test 5 and test 3. It is indicated that the wave flume tests have a very good repeatability. From the perspective of displacement, the horizontal and vertical displacement of the breakwater are only 0.05 mm and 0.02mm (as listed in Table 6), respectively in test 3, which are basically the same as that recorded in test 5. It means that the revetment breakwater is stable under the tsunami wave impacting in test 3, even though it is built on the relatively

Fig. 17 Comparison of the impact force on structures **A** and **B** measured in test 5 (without accropodes) and test 6 (with accropodes)

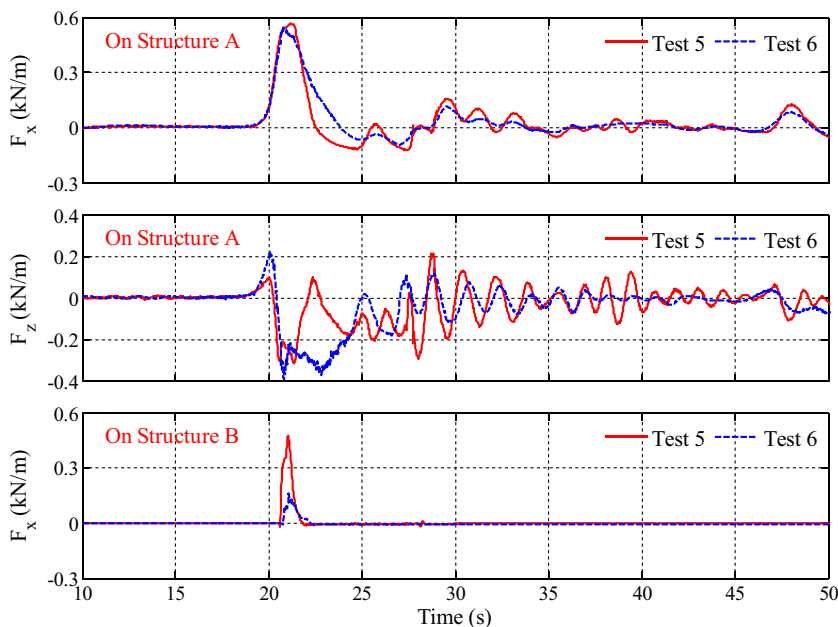
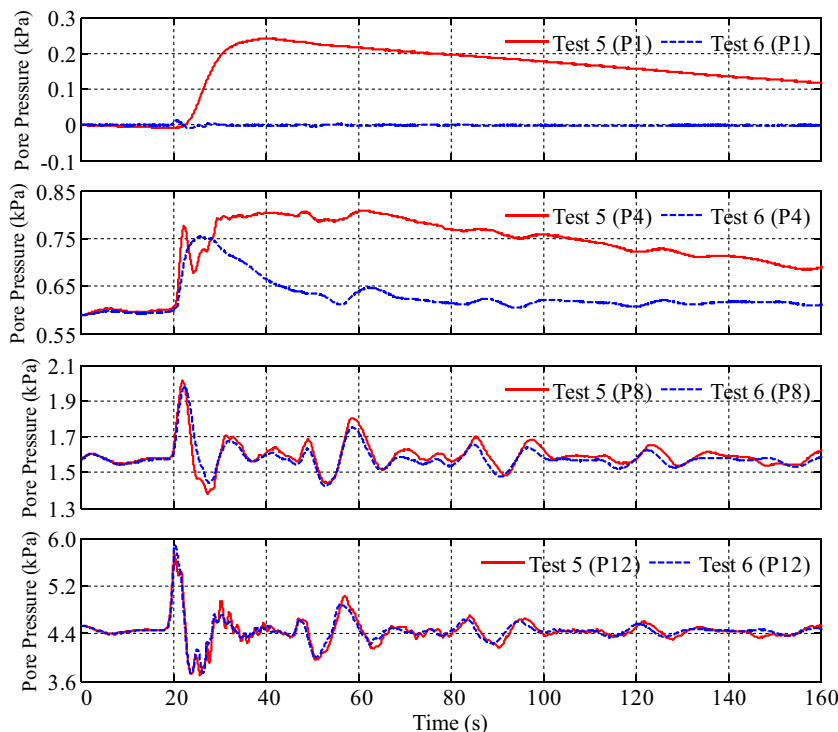


Fig. 18 Comparison of the pore pressure at P1, P4, P8, and P12 recorded in test 5 (without accropodes) and test 6 (with accropodes)



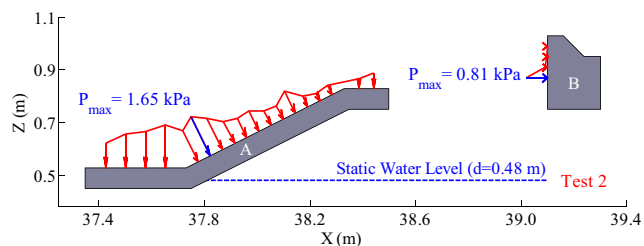


Fig. 19 Distribution of the maximum wave impact on the revetment breakwater recorded in test 2 ($d = 0.48$ m)

loose coral sand foundation. Overall, the density of foundation has minor effect on the stability of the revetment breakwater under tsunami impacting. However, this recognition would be inappropriate for random severe ocean waves. Further laboratory tests will be conducted on this issue in the future.

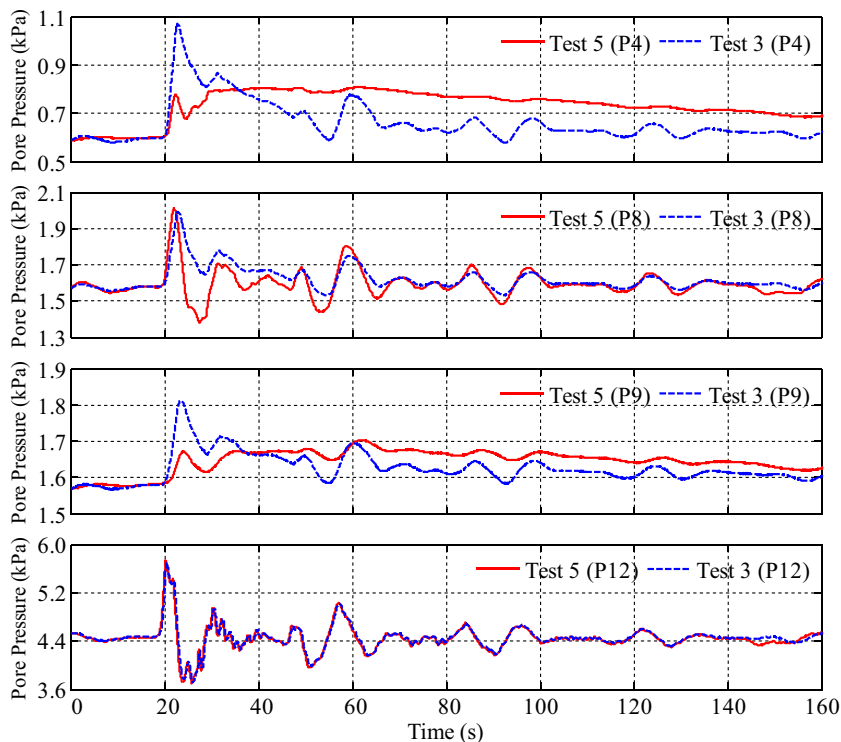
Conclusion

In this study, taking the reclamation engineering in the South China Sea as the background, several wave flume experiments (geometrical similarity scale is set as 1:10) are performed to study the dynamics and the stability of a reclaimed coral sand foundation and the revetment breakwater built on it under the tsunami wave impacting. Due to the fact that there is only one peak impacting for a tsunami wave, the following recognitions would be not applicable to the cases in which continuous

wave impacting is applied on the breakwater. The main conclusions are drawn as follows:

- (1) Maximal horizontal and vertical displacement of the revetment breakwater are only 0.05 mm and 0.1 mm, respectively. Besides, there is no large deformation observed in the reclaimed coral sand foundation during testing. The revetment breakwater is stable under the tsunami wave impacting due to the fact that the reclaimed coral sand foundation behind the revetment breakwater can provide strong passive soil pressure.
- (2) The excess pore pressure in the reclaimed coral calcareous foundation has a maximal value of 1.5 kPa. This excess pore pressure could not cause liquefaction in the coral sand foundation.
- (3) The overtopped water would be a potential threat for the vegetation behind the breakwater, as well as for the desalinated underground water in these reclaimed lands.
- (4) Accropodes could significantly enhance the stability of the revetment breakwater under impacting of tsunami. Tsunami waves will bring less threat to the stability of the revetment breakwater at low tide level. Dry density of foundation has minor effect on the stability of the revetment breakwater under tsunami wave impacting.
- (5) It should be noted that the permeability and the deformation modulus of the coral sand foundation in the physical model must have been slightly amplified comparing with that in prototype foundation due to the fact that the geo-

Fig. 20 Comparison of the pore pressure measured in test 5 ($\rho_d = 1500\text{kg/m}^3$) and test 3 ($\rho_d = 1320\text{kg/m}^3$)



metric model scale 1:10 has not been applied to the granular foundation materials. As a result, the magnitude of the displacement of the revetment breakwater and the peak pore pressure in the coral sand foundation recorded in the physic model test would be underestimated relative to that in the prototype model at the engineering in-sites in the South China Sea. Therefore, the analysis on the pore pressure in the coral sand foundation and on the revetment breakwater's displacement presented in this work needs to be understood adopting a dialectical way.

- (6) It is well known that the calcareous coral sands would be different from region to region in the globe. Therefore, the findings and the analysis presented in this study are only applicable to the reclamation project in the South China Sea.

Funding This work received funding support from the National Natural Science Foundation of China, Grant No. 51879257, as well as funding support from the "Strategic Priority Research Program of the Chinese Academy of Sciences," Grant No. XDA13010202.

References

- Chávez V, Mendoza E, Silva R, Silva A, Losada M (2017) An experimental method to verify the failure of coastal structures by wave induced liquefaction of clayey soils. *Coast Eng* 123:1–10
- Esteban M, Thao ND, Takagi H, Shibayama T. (2008) Laboratory experiments on the sliding failure of a caisson breakwater subjected to solitary wave attack. In Proceedings of the Eighth ISOPE Pacific/Asia Offshore Mechanics Symposium, Bangkok, Thailand, 10–14 November.
- Esteban M, Thao ND, Takagi H, Shibayama T (2009) Pressure exerted by a solitary wave on the rubble mound foundation of an armoured caisson breakwater. In Proceedings of the 19th International Offshore and Polar Engineering Conference, Osaka, Japan, 21–26 June.
- Esteban M, Morikubo I, Shibayama T, Muñoz RA, Mikami T, Thao ND, Ohira K, Ohtani A (2012) Stability of rubble mound breakwaters against solitary waves. In Proceedings of the 33rd International Conference on Coastal Engineering, Santander, Spain, 1–6 July.
- Gao R, Ye JH (2019) Experimental investigation on the dynamic characteristics of calcareous sand from the reclaimed coral reef islands in the South China Sea. *Rock Soil Mech* 40(10):3897–3896
- Gu C (2011) Geographical report of 311 earthquake in Japan. *Acta Geograph Sin* 66(6):853–861
- Guler HG, Baykal C, Arikawa T, Yalciner AC (2018) Numerical assessment of tsunami attack on a rubble mound breakwater using OpenFOAM®. *Appl Ocean Res* 72:76–91
- Guler HG, Arikawa T, Oei T, Yalciner AC (2015) Performance of rubble mound breakwaters under tsunami attack, a case study: Haydarpaşa Port, Istanbul, Turkey. *Coast Eng* 104:43–53
- Grimshaw R (1971) The solitary wave in water of variable depth. Part 2. *J Fluid Mech* 46(03):611
- Hanzawa M, Matsumoto A, Tanaka H (2012a) Stability of wave-dissipating concrete blocks of detached breakwaters against tsunami. ICCE
- Hanzawa M, Matsumoto A, Tanaka H (2012b) Applicability of cadmasurf to evaluate detached breakwater effects on solitary tsunami wave reduction. *Earth, Planets and Space* 64(10):955–964
- He SH, Ding Z, Xia TD, Zhou WH, Gan XL, Chen YZ, Xia F (2020a) Long-term behaviour and degradation of calcareous sand under cyclic loading. *Eng Geol* 276:105756
- He SH, Zhang QF, Ding Z, Xia TD, Gan XL (2020b) Experimental and estimation studies of resilient modulus of marine coral sand under cyclic loading. *J Mar Sci Eng* 8(4):287
- Ikeno M, Mori N, Tanaka H (2001) Experimental study on tsunami force and impulsive force by a drifter under breaking bore like Tsunamis. *Coast Eng J* 48:846–850
- Ikeno M, Tanaka H (2003) Experimental study on impulse force of drift body and tsunami running up to land. *Ann J Coast Eng* 50:721–725
- Imase T, Maeda K, Miyake M, Sawada Y, Sumida H, Tsurugasaki K (2012) Destabilization of a caisson type breakwater by scouring and seepage failure of the seabed due to a tsunami. Proc. of. In: 6th Int. Conf. on Scour and Erosion, pp 807–814
- JTS154-1-2011 (2011) Code of design and construction of breakwaters. Ministry of transport of China. (in Chinese)
- Kirby S, Geist E, Lee W H K (2006). Great earthquake tsunami sources: empiricism and beyond. USGS Tsunami Sources Workshop.
- Mikami T, Kinoshita M, Matsuba S, Watanabe S, Shibayama T (2015) Detached breakwaters effects on tsunamis around coastal dykes. *Procedia Eng* 116:422–427
- Miyake M, Sumida H, Maeda K, Sakai H, Imase T (2009) Development of centrifuge modelling for tsunami and its application to stability of a caisson type breakwater. *Ann J Civil Eng Ocean* 25:87–92 (in Japanese)
- Mizutani S, Imamura F (2000) Hydraulic experimental study on wave force of a bore acting on a structure. *Coast Eng J* 47:946–950
- Ranghieri F, Ishiwatari M (2008) Learning from megadisasters: lessons from the Great East Japan Earthquake. World Bank Publications, Washington, DC, USA
- Rossetto T, Allsop W, Charvet I, Robinson DI (2011) Physical modelling of tsunami using a new pneumatic wave generator. *Coast Eng* 58(6): 517–527
- Satake K, Aung TT, Sawai Y, Okamura Y, Win KS, Swe W, Oo TZ (2005) Report on post tsunami survey along the Myanmar Coast for the December 2004 Sumatra 2 Andaman earth quake. In: 161 - 188
- Sun L, Zhou X, Huang W, Liu X, Yan H, Xie Z, Yang W (2013) Preliminary evidence for a 1000-year-old tsunami in the South China Sea. *Sci Rep* 3:1655
- Sumer BM (2009) Liquefaction around marine structures. In: Coastal Structures 2007 - 5th Coastal Structures International Conference, p CST07
- Sassa S, Takahashi H, Morikawa Y, Takano D (2016) Effect of overflow and seepage coupling on tsunami-induced instability of caisson breakwaters. *Coast Eng* 117:157–165
- Sawada Y, Miyake M (2015) Numerical analysis on stability of caisson-type breakwaters under tsunami-induced seepage. *Transp Infrastruct Geotechnol* 2(3):120–138
- Synolakis C E (1999) Exact solutions of the shallow-water wave equations. *Advances In Coastal and Ocean Engineering*. pp 61–131
- Tadepalli S, Synolakis CE (1994) The run-up of N-waves on sloping beaches. *Pro R Soc London A*445:99–112
- Tadepalli S, Synolakis CE (1996) Model for the leading waves of tsunamis. *Phys Rev Lett* 77(10):2141–2144
- Takagi H, Bricker JD (2014) Assessment of the effectiveness of general breakwaters in reducing tsunami inundation in Ishinomaki. *Coast Eng J* 56(04):1450018
- Teh TC, Palmer AC, Damgaard JS (2003) Experimental study of marine pipeline on unstable and liquefied seabed. *Coast Eng* 50(1–2):1–17
- Tanimoto L, Tsuruya K, Nakano S (1984) Tsunami force of Nihonkai-Chubu Earthquake in 1983 and cause of revetment damage. In

- Proceedings of the 31st Japanese Conference on Coastal Engineering, Tokyo, Japan, 13–14 April
- Takahashi H, Sassa S, Morikawa Y, Takano D, Maruyama K (2014) Stability of caisson-type breakwater foundation under tsunami-induced seepage. *Soils Found* 54(4):789–805
- Wang X, Zhu CQ, Wang XZ, Qin Y (2019) Study of dilatancy behaviors of calcareous soils in a triaxial test. *Mar Georesour Geotechnol* 37(9):1057–1070
- Ye JH, Jeng DS, Wang R, Zhu CQ (2013a) Validation of a 2-D semi-coupled numerical model for fluid–structure–seabed interaction. *J Fluids Struct* 42:333–357
- Ye JH, Jeng DS, Wang R, Zhu CQ (2013b) A 3-D semi-coupled numerical model for fluid–structures–seabed-interaction (FSSI-CAS 3D): model and verification. *J Fluids Struct* 40:148–162
- Ye JH, Jeng DS, Wang R, Zhu CQ (2013c) Numerical study of the stability of breakwater built on a sloped porous seabed under tsunami loading. *Appl Math Model* 37(23):9575–9590
- Zhang Y, Ye JH (2021) Physical modelling of the stability of a revetment breakwater built on reclaimed coral calcareous sand foundation in the South China Sea-random waves and dense foundation. *Ocean Eng* 219:108384
- Zhou Q, Adams WM (1986) Tsunamigenic earthquakes in China, 1831 BC to 1980 AD. *Sci Tsunami Hazards* 4(3):131–148